BOLLETTINO DI GEOFISICA TEORICA ED APPLICATA VOL. XXXV, N. 137-138 - MARCH-JUNE 1993

A. LOZEJ and I. TABACCO

RADIO ECHO SOUNDING ON STRANDLINE GLACIER, TERRA NOVA BAY (ANTARCTICA)

Abstract. This paper is a report of a Radio Echo Sounding, R.E.S. survey (recently renamed as Ground Penetrating Radar, G.P.R.), carried out on the Strandline Glacier (Terra Nova Bay) during the Italian Antarctic expedition 1988-89. The Strandline Glacier is a local dry-based glacier of particular interest because its fluctuations can be related to climatic variations. The R.E.S. profile allowed us to determine the thickness of the ice cover, the morphology of the bedrock and to distinguish geometrical trends and discontinuities in the ice cover. R.E.S. profiles will be repeated in the future to study variations of ice thickness and to evaluate mass balance.

INTRODUCTION

Strandline Glacier is a cold (dry-based) local glacier located at the southernmost margin of Gerlache Inlet in Tethys Bay, Northern Victoria Land, Antarctica (Fig. 1). It is the only glacier in the area which terminates with an ice cliff resting on Holocene raised beaches (Baroni and Orombelli, 1987; Carmignani et al., 1988).

Local glaciers respond sensitively to short term climatic and environmental changes, and the study of their fluctuations is particularly important because they may be related to climatic variations.

Topographic surveys and control measurements have been carried out since 1986 and used to evidence a slight retreat of Strandline Glacier (Baroni, 1987). However, mass balance calculations have not yet been performed because the volumes are not known. For this reason, R.E.S. profiles were done to determine the thickness of the ice cover, and the morphology of the bedrock (Nye, 1975; Paren and Robin, 1975; Robin, 1975).

THEORETICAL OUTLINE OF THE R.E.S. TECHNIQUE

The main objective of R.E.S. survey is the location of buried electromagnetic reflectors. It may be useful to recall the most important equations and parameters that control this technique and to indicate their applications and modifications in ice exploration.

The propagation of electromagnetic waves is described by Maxwell's equations:

$$\nabla^2 E=\gamma^2 E \quad ; \quad \nabla^2 H=\gamma^2 H, \tag{1}$$

where

Manuscript received September 30, 1991; accepted September 28, 1992.

Università di Milano, Dip. Scienze della Terra, Via Cicognara 7, 20129 Milano, Italy.

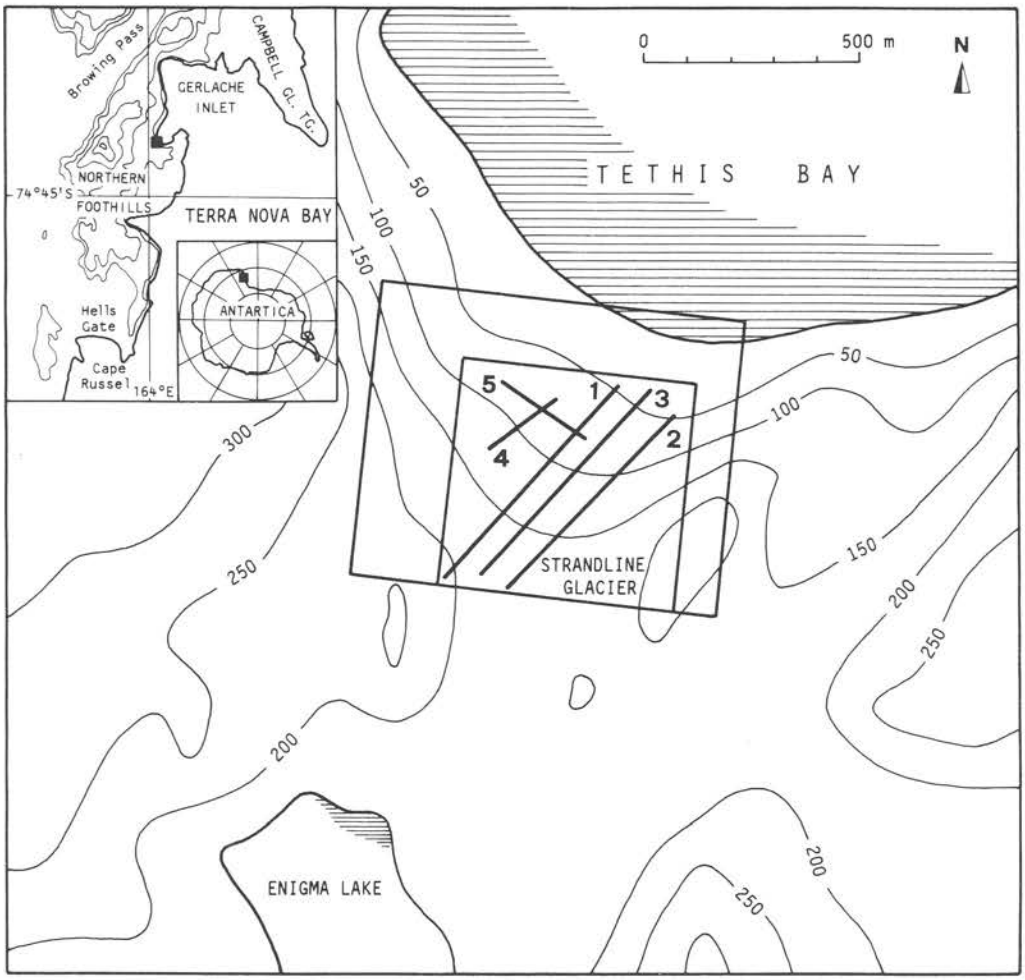

Fig. 1 — Location map and working area of Strandline Glacier.

$$\gamma^2 = j\,\omega\,\mu\cdot(\sigma + j\,\omega\,\epsilon), \tag{2}$$

with

$j = \sqrt{-1}$,

$\omega = 2\,\pi\,f$ = *angular frequency*,

$\mu = \mu_o \cdot \mu_r$ = *magnetic permeability*,

$\epsilon = \epsilon_o \cdot \epsilon_r$ = *electric permittivity (dielectric constant)*,

σ = *conductivity*.

The coefficient γ is a complex number whose real and imaginary parts represent the attenuation factor and phase coefficient, respectively.

Letting

$$\gamma=\alpha+j\,\beta\,, \tag{3}$$

from eqn. (2) we obtain

$$\alpha=\omega\cdot\left\{\frac{\mu\epsilon}{2}\cdot\left[\left(1+\left(\frac{\sigma}{\omega\epsilon}\right)^2\right)^{1/2}-1\right]\right\}^{1/2}, \tag{4a}$$

$$\beta=\omega\cdot\left\{\frac{\mu\epsilon}{2}\cdot\left[\left(1+\left(\frac{\sigma}{\omega\epsilon}\right)^2\right)^{1/2}+1\right]\right\}^{1/2}. \tag{4b}$$

Considering plane waves, the electric field E (x, t) at any point x and at time t may be expressed by the following relation:

$$E\ (x,\ t)=E_o\cdot e^{-\alpha x}\cdot e^{j\,(\omega t-\beta x)}. \tag{5}$$

In this equation, the term $e^{-\alpha x}$ represents the attenuation factor; the phase velocity is given by

$$v=\frac{\omega}{\beta}\,. \tag{6}$$

Reflections at the boundary of two media are determined by variations of the intrinsic impedence Z given by the equation

$$|Z|=\left(\frac{\mu}{\epsilon}\right)^{1/2}:\left[1+\left(\frac{\sigma}{\omega\epsilon}\right)^2\right]^{-1/4}. \tag{7}$$

The reflection coefficient R is defined as

$$R=\frac{Z_2-Z_1}{Z_2+Z_1}. \tag{8}$$

The propagation and reflections of electromagnetic waves are therefore determined by four parameters ω, σ, μ, and ϵ.

In the case of ice surveys, we can make some simplifications (Berry, 1975; Page and Ramseier, 1975; Bentley, 1982; Bogordosky et al., 1985): since the ice electrical conductivity $\sigma<10^{-3}$ mho/m, the value of the ratio $\left(\frac{\sigma}{\omega\epsilon}\right)$ is $<<1$ for frequencies >80 MHz, and thus the term under the inner square root in eqns. (4a) and (4b) is almost equal 1; furthermore, considering that for ice $\mu=\mu_o$, we can rewrite the eqns. (4), (5), (6) and (7):

$$\alpha\simeq 0 \quad ; \quad \beta\simeq\omega\cdot\sqrt{\mu_o}\,\epsilon, \tag{4'}$$

$$E\ (x,\ t)\simeq E_o\cdot e^{j\,(\omega\,(t-x\sqrt{\mu_o\epsilon}))}, \tag{5'}$$

$$v\simeq\frac{c}{\sqrt{\epsilon_r}}\,. \tag{6'}$$

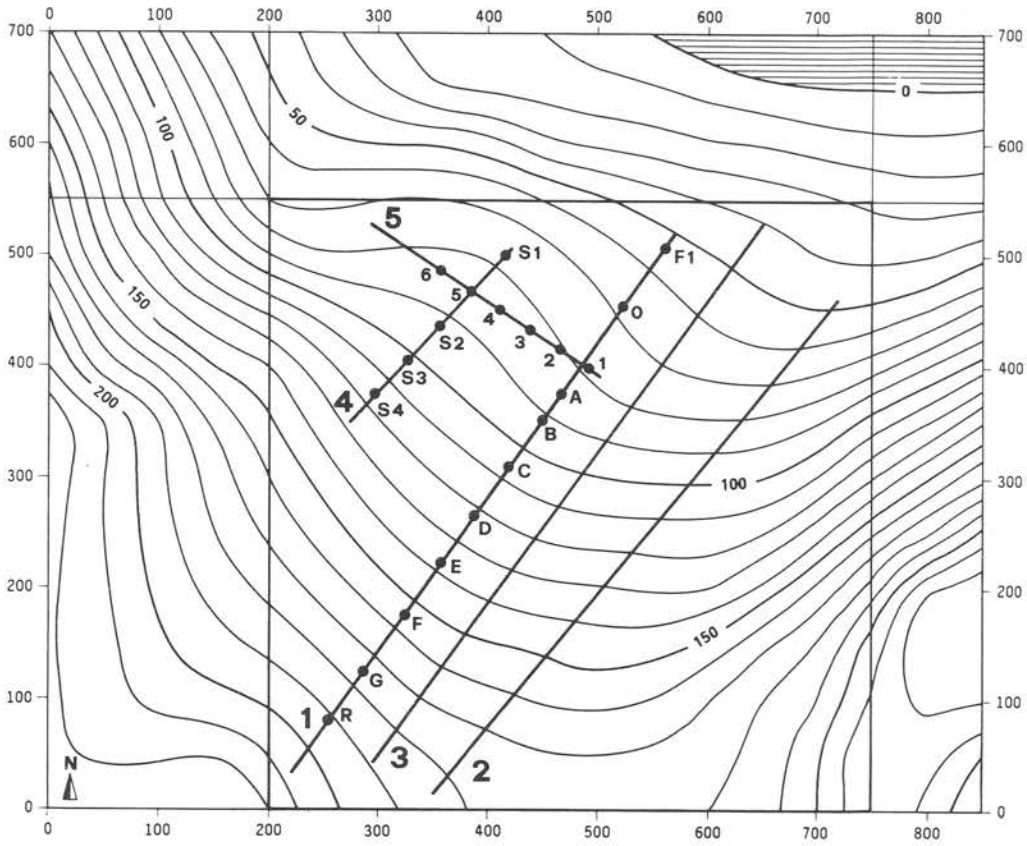

Fig. 2 — Location map of R.E.S. profile and Strandline topography.

$$|Z| \simeq \sqrt{\frac{\mu_o}{\epsilon}} \quad . \tag{7'}$$

We conclude that in ice surveys, the attenuation coefficient is very low for frequencies greater than 80 MHz, and thus the velocity of e.m. waves is determined only by the ice dielectric constant.

In this work, we did not take measurements of ice dielectric constant; for interpretation, we used the value $\epsilon_r = 3.3$ according to the literature values (Paterson, 1981; Kovacs and Morey, 1985; Ulriksen, 1982).

The dielectric constant of bedrock (granite) is greater than 5-6, the impedence contrast between ice and bedrock is quite high and the boundary represents a potential electromagnetic reflector. It is also possible to obtain reflections from the boundary between snow or firn cover ($\epsilon_r < 2.5$, Ulriksen, 1982) and the ice surface. The possibility of getting reflections from within the ice cover is more problematic because impedence contrasts are low: however, the presence of thin lithic deposits within the ice sheet may increase the impedence contrast.

EXPERIMENTAL SURVEY

Strandline glacier is located at the southern side of Tethys bay, which corresponds to the coordinates 74°41' S and 164°06' E. Its maximum length is about 600 m and the width is less than 500 m; its elevation ranges from sea level, where the glacier terminus is represented by a cliff 25 m high, to 200 m a.s.l. The glacier surface slope is about 25%, but in its highest

part the slope may be over 30%. Small transversal crevasses are present where the slope of the glacier changes.

The morphology of the glacier constrained the position of the radar profiles. Therefore, only four longitudinal and one transversal profiles were taken (Fig. 2).

Acquisition was done with an electromagnetic pulse generator, a transmitter-receiver antenna and a central unit with controlling and recording functions. A continuous profile at zero offset was obtained by towing the antenna at a constant velocity (about 2 km/h). In this work, we used an antenna centered at a frequency of 80 MHz. The radio signals transformed into audio frequencies are recorded by an AD converter and subsequently processed to give profiles which are similar to seismic profiles.

Data were acquired using two different time scales (1000 and 1500 ns, twt) in order to get information both from the deepest reflectors and from intermediate and superficial bodies. The Table summarizes data relative to the profiles which were taken. Range, dimensions of files in megabytes (MB), total number of scans, lengths of the profiles and number of scans per meter are here reported.

Table - Data profile: range, length and scan density.

Profile		Range (ns)	MB	scan	m	scan/m
1	S-N	1500	10.35	20210	587	34.4
	N-S	1000	8.13	15889	587	27.1
2	S-N	1000	10.43	20370	581	35.1
3	N-S	1500	7.79	15209	602	25.3
4	N-S	1000	3.59	7007	214	32.7
5	E-W	1000	2.72	5310	246	21.6
	W-E	1500	2.88	5622	246	22.8

The number of scans per meter changes if the towing speed of the antenna varies as a consequence of surface morphology: values given in the Table represent a mean for each profile. The horizontal scale was normalized by using the topographic position of markers set up along the profile.

An example of the results of the main processing steps is described for the NW-SE profile 5. Fig. 3a shows the unprocessed film section presenting noise in the vertical direction (time domain) and in the horizontal direction (space domain).

By means of vertical filtering (triangular filter) (Fig. 3b) and subsequent horizontal filtering, the noise was greatly attenuated (Fig. 3c).

INTERPRETATION

The processed film sections were interpretated with the usual methods used in zero offset reflection surveying. Reduction to topographic surface, migration and time-depth conversion were carried out by line-drawing interpretation, using the electromagnetic wave velocity given by eqn. (6'). With a value of $\epsilon_r = 3.3$, the time scale on the film section (twt) corresponds to a depth scale 100 ns = 8.25 m.

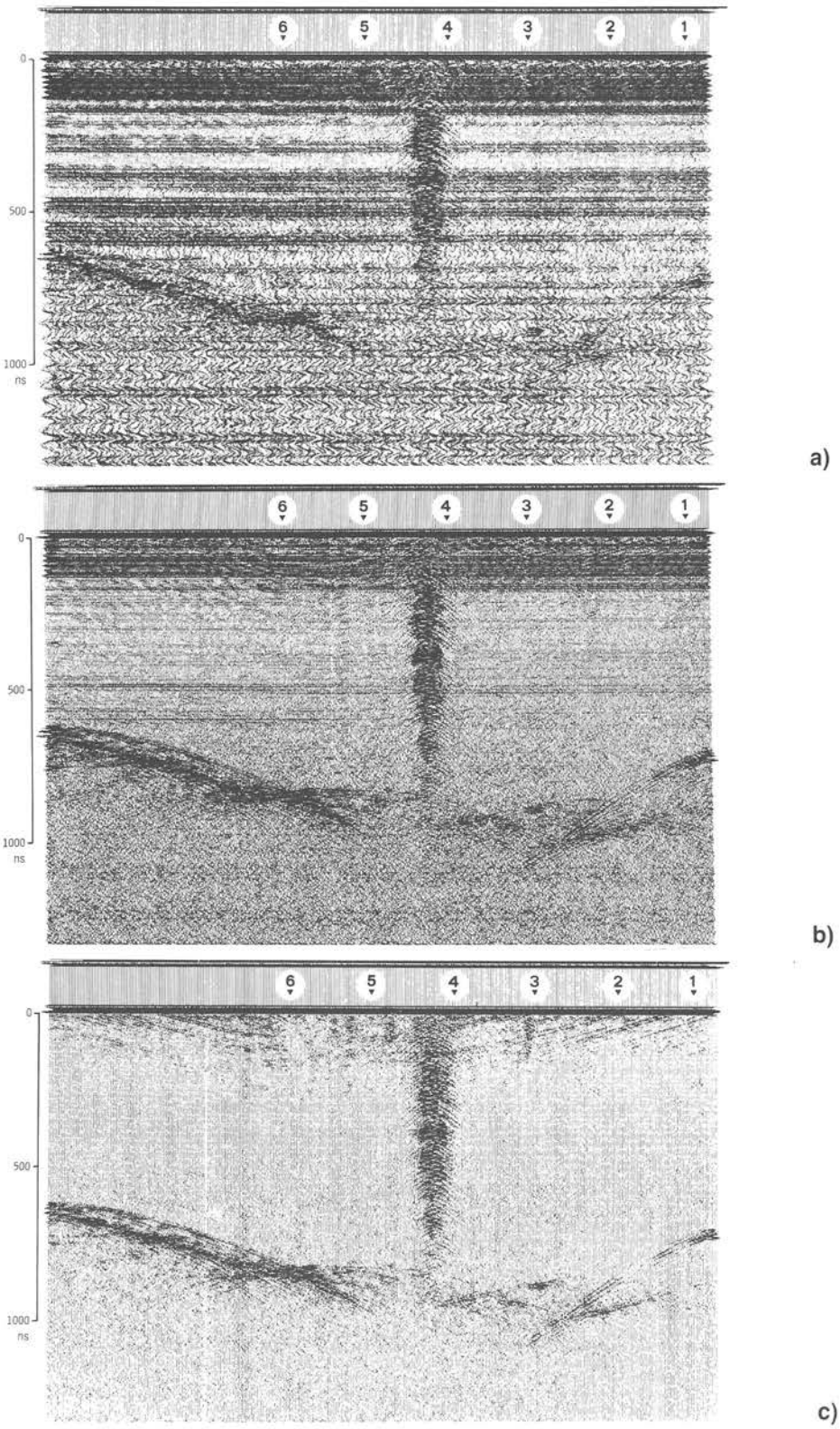

Fig. 3 — Profile 5 NW-SE film sections, range 1500 ns: a) unprocessed; b) vertical filtered; c) horizontal filtered.

Profile 1

This profile was taken in both the NNE-SSW and SSW-NNE directions (Figs. 4a and 4b) by using time ranges of 1000 and 1500 ns, respectively. The topographic trend of the profile goes from an elevation of 50 m a.s.l. north to 200 m a.s.l. south. Between markers F1 and A, and from marker C to the south, a deep continuous high energy reflector can be observed; between markers A and C, the reflector becomes very weak. Some local slope variations generate diffraction patterns.

The weakening of reflections in the central part of the profile does not mean that the reflector stops: in fact, abrupt changes in the inclination of the slope may produce interference and superposition of diffracted and reflected impulses. Thus, the reflector is considered as continuous. Reflection amplitude, indicative of a strong impedence contrast, and the morphology of the reflector (outcropping in the southern part) suggest its interpretation as the ice bedrock interface (Harrison, 1970, 1973; Oswald, 1975). Within the ice cover it is possible to observe some synclinal reflections which stop abruptly in the central part of the glacier. These have been interpreted as foliations within the ice (Clough, 1977; Dowdeswell et al., 1984). Between markers E and F can be observed intermediate reflections of high energy, strong inclination and angular unconformity with respect to the bedrock. The glaciological interpretation of these features is given in the conclusions.

Fig. 4c shows the depth section that was obtained by using a constant value of ϵ_r even if examination of the film sections may suggest the presence of firn and variations within the ice cover. However, it must be observed that different choices of the dielectric constant result in depth variations over a range less than +/—5%.

Profile 2

This profile (Figs. 5a and 5b) is located at the eastern shoulder of the glacier. Within the cover, it is possible to observe some isolated diffractions which can be ascribed either to the unevennes of the bedrock surface or to the presence of isolated bodies of variable size within the ice sheet.

Profile 3

This profile (Figs. 6a and 6b) confirms all the main elements observed and described for profile 1. The deepest reflector has the same trend but shorter reflection time with respect to profile 1. The presence of both foliations and an intermediate reflector is also confirmed.

Profile 4

This profile is only roughly located because of the strong inclination of this part of the glacier which did not allow measurements along a straight line. However, all the main elements are confirmed (Figs. 7a and 7b): foliations with synclinal trend and the loss of bedrock reflections in the deepest central part.

A crevasse showing typical diffractions can also be observed (Kovacs and Abele, 1974).

Profile 5

Figs. 8 and 3 show SE-NW and NW-SE film sections recorded with time ranges of 1000 and 1500 ns, respectively. The relative depth section is also shown in Fig. 8b. We can observe a deep reflector of high energy and regular trend. This reflector, corresponding to the ice-bedrock boundary, deepens towards the centre where it has an irregular trend and shows a diffraction pattern.

This roughness can be ascribed to the presence of debris on the abrasion surface. Towards the surface, it is possible to observe diffractions caused by a crevasse outcropping in the central part of the profile. In the same area, there are other minor crevasses and a large number of foliations with synclinal trend and axis normal to the longitudinal profiles.

The profile cross-cuts lines 1, 3 and 4 and the depths of the bedrock are confirmed at the intersections.

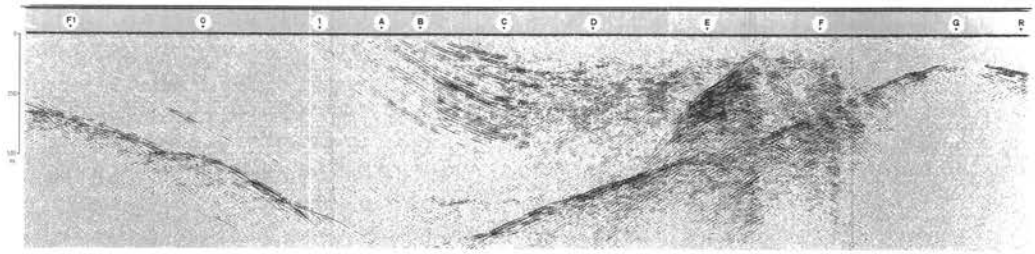

a)

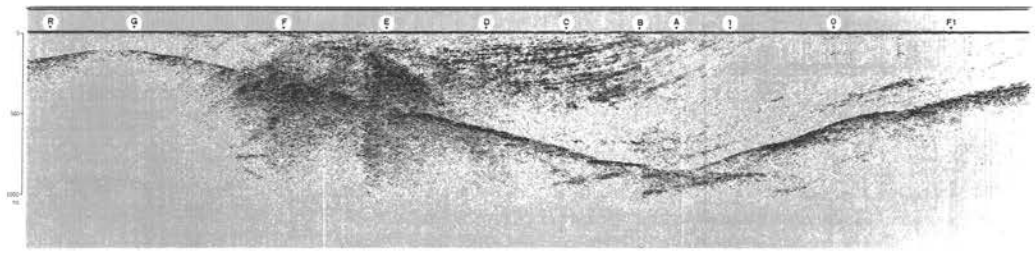

b)

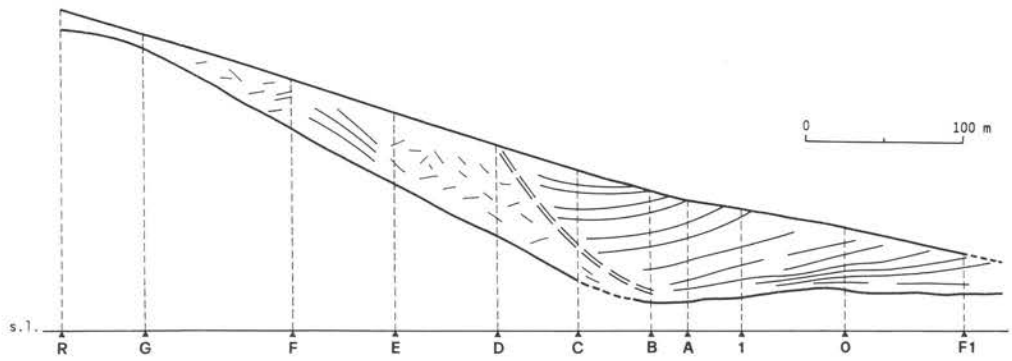

c)

Fig. 4 — Profile 1: a) NNE-SSW film section, range 1000 ns; b) SSW-NNE film section, range 1500 ns; c) depth section.

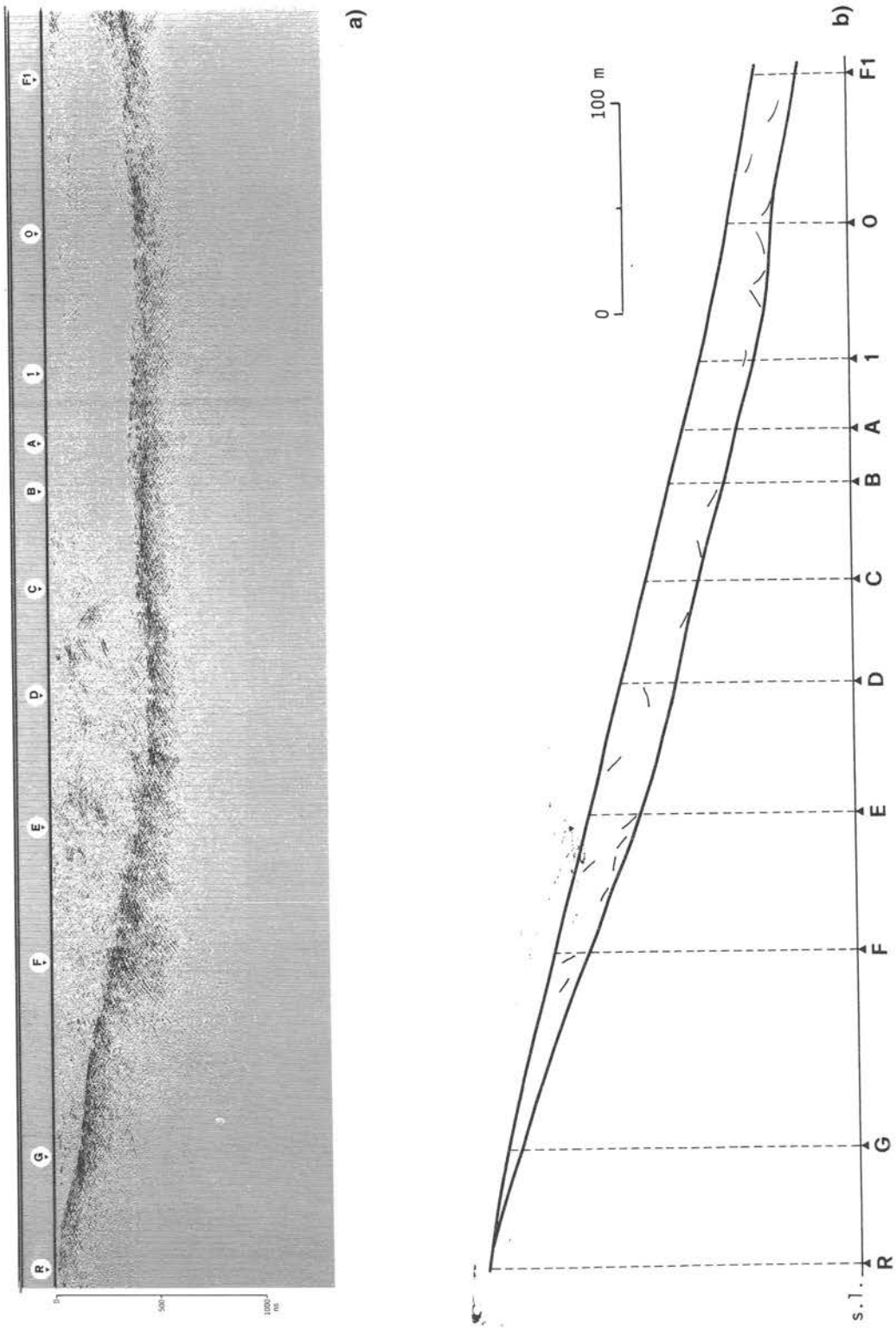

Fig. 5 — Profile 2: a) NNE-SSW film section, range 1000 ns; b) depth section.

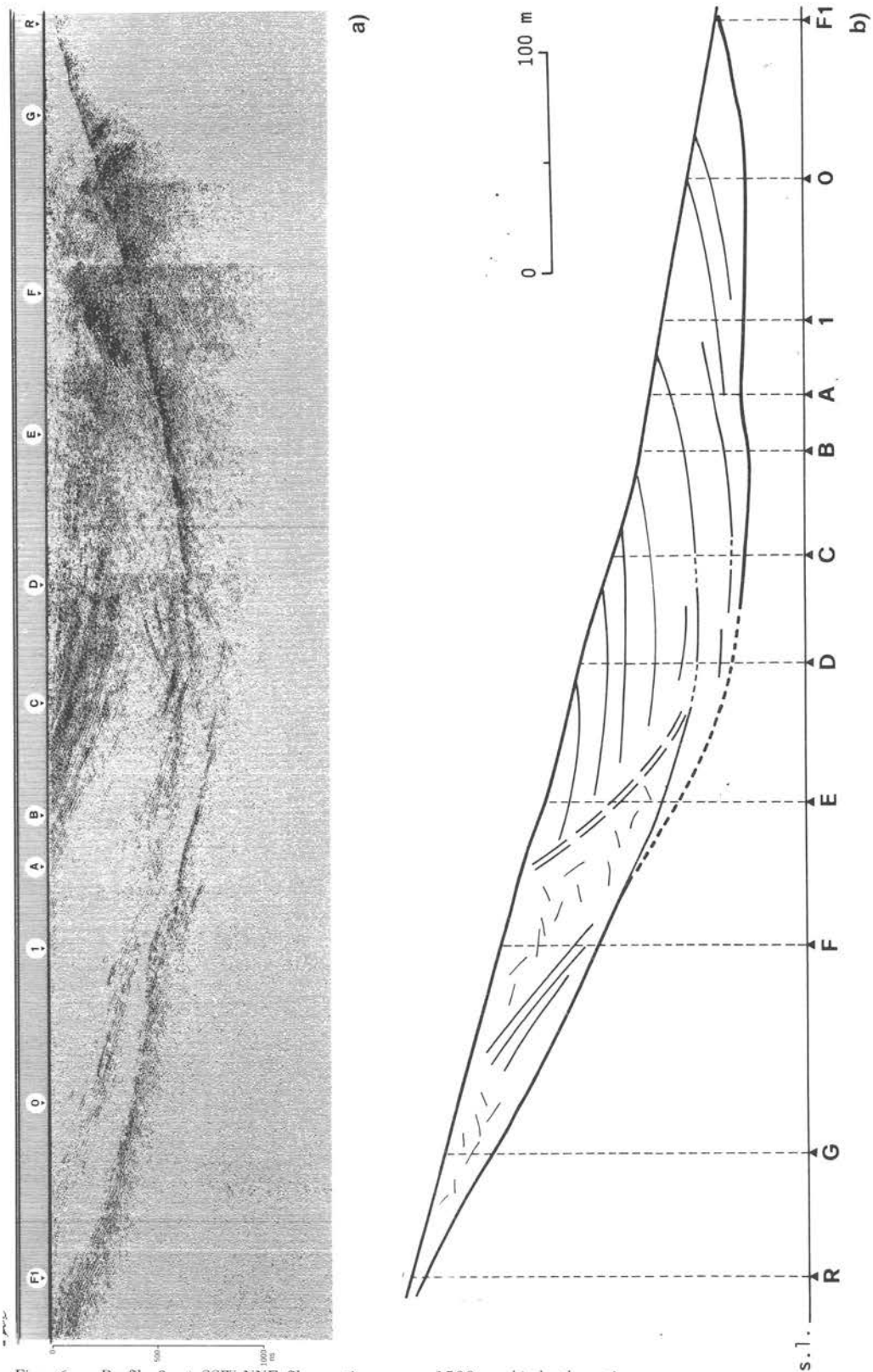

Fig. 6 — Profile 3: a) SSW-NNE film section, range 1500 ns; b) depth section.

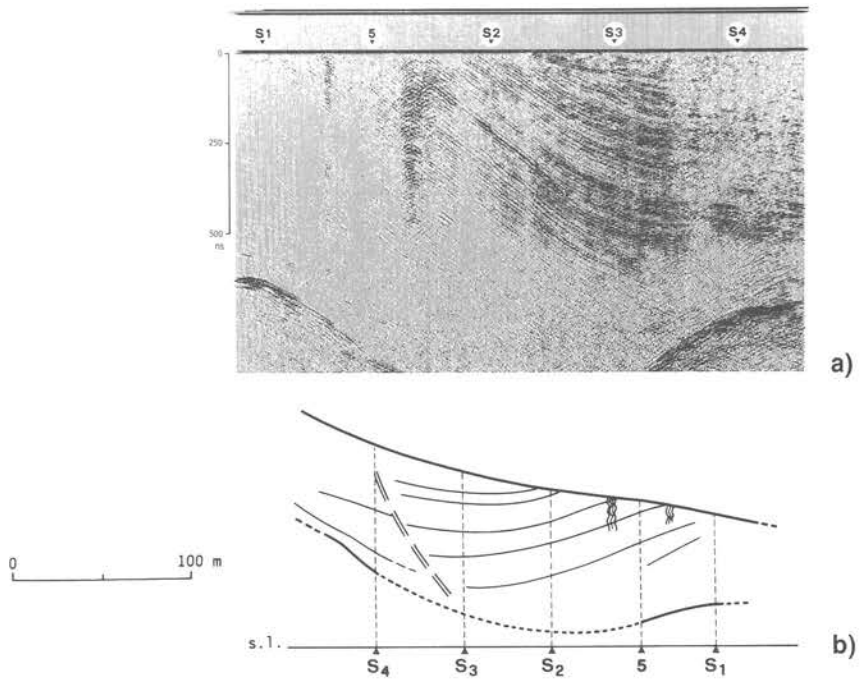

Fig. 7 — Profile 4: a) SSW-NNE film section, range 1000 ns; b) depth section.

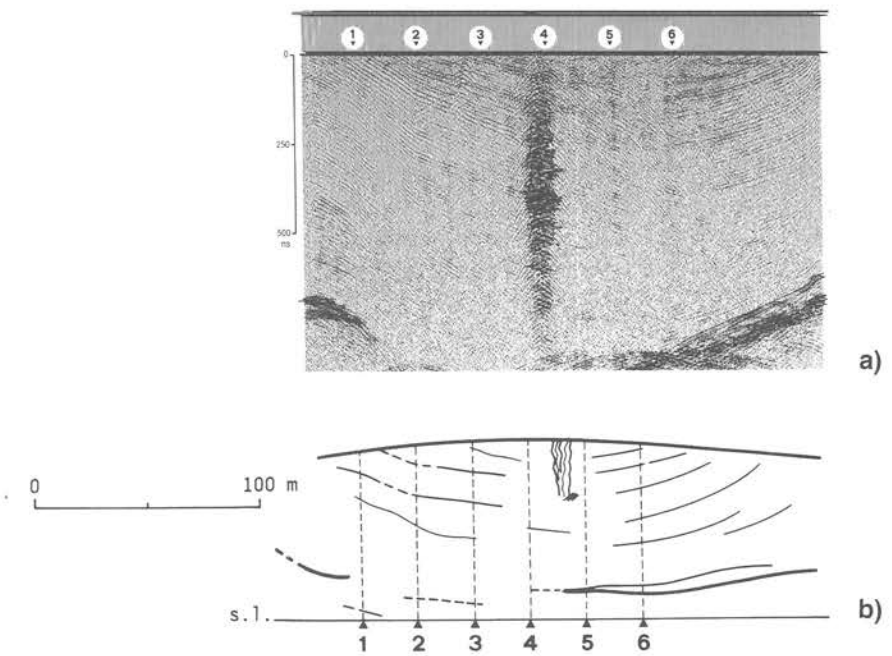

Fig. 8 — Profile 5: a) SE-NW film section, range 1000 ns; b) depth section.

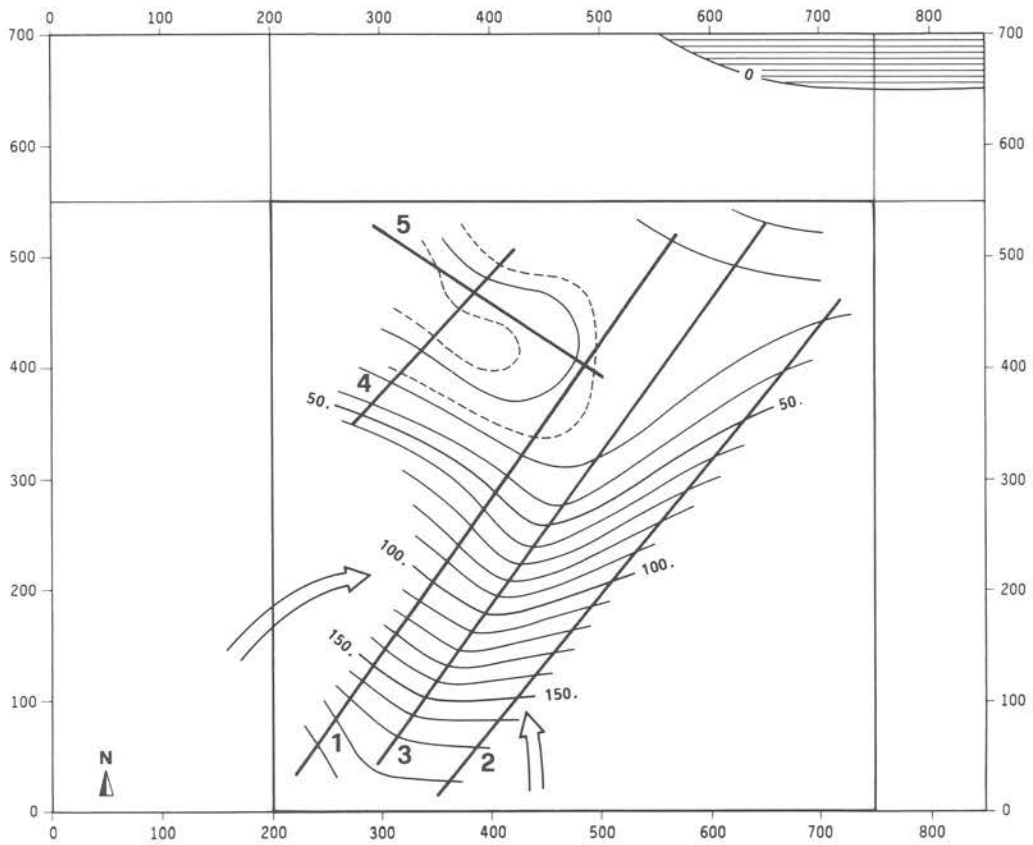

Fig. 9 — Isobath map of bedrock and ice-flow line trend.

CONCLUSIONS

By analyzing all the profiles, three different zones of ice cover can be distinguished.

- The first zone, located in the lower part of the glacier, is characterized by closely spaced reflections starting from the surface and going almost all the way down to bedrock. The topographic pattern of these reflections evidences a synclinal trend with the main axis following the maximum inclination direction, and a secondary less inclined axis perpendicular to it. Such reflections are interpreted as due to ice foliations.

- A second zone, in the upper part of the glacier, characterized by the presence of intermediate reflectors with angular unconformities at both the base and the topographic surface. Such reflectors do not screen reflections from the deeper bedrock and are interpreted as discontinuities in the ice cover; the amplitude of the reflections and their stratifications may suggest the presence of lithic material deposited at the surface of the body during successive phases. Following Chinn et al. (1989), they may be considered as a fossil ice body.

- The third zone, intermediate with respect to the preceding ones, has different characteristics: no continuous reflections have been observed, but only small stretchs randomly distributed within the ice cover that are indicative of compressive phenomena.

In Fig. 9 the isobaths of the bedrock are mapped; two different areas can be distinguished: a southern one characterized by strong inclination (50%), and a northern one almost flat and slightly concave at the centre where it reachs its minimum elevation (lower than 15 m a.s.l.). The bedrock and topographic morphology in the upper part of the glacier are indicative of

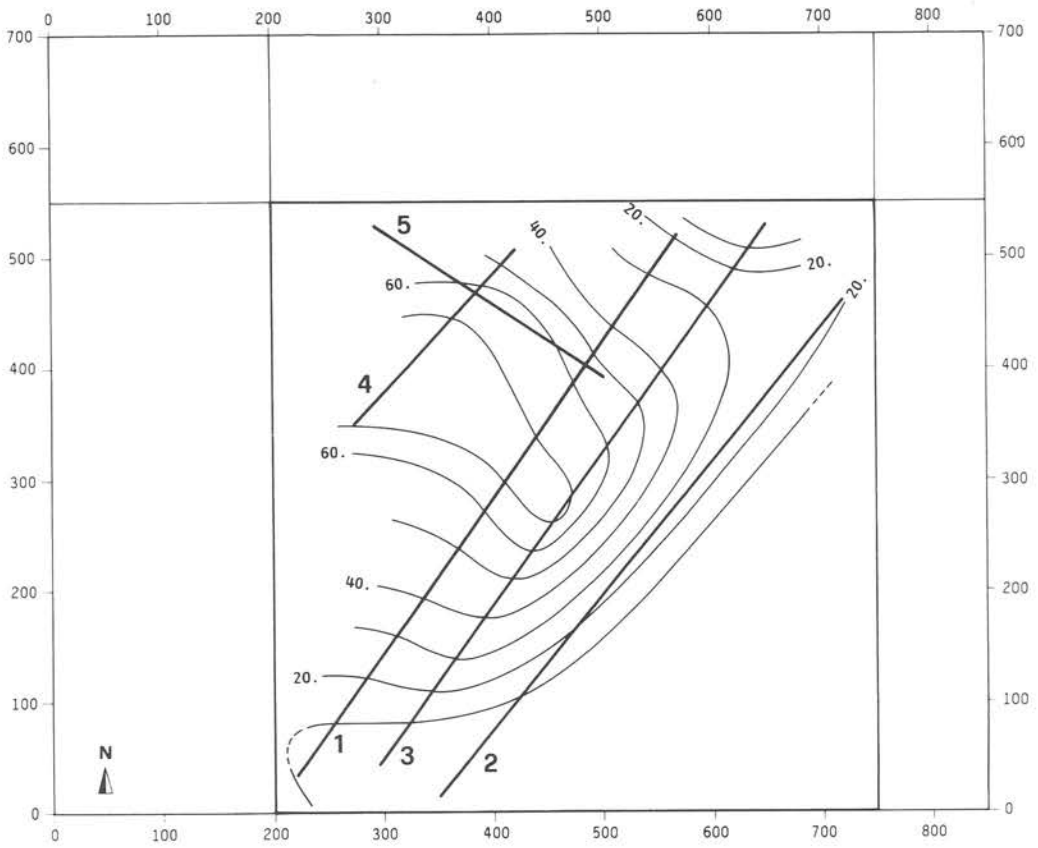

Fig. 10 — Isopach map of ice cover.

a division of the main ice flow into two different lines that meet together in the lower area. This hypothesis is coherent with the features of the fossil ice body and with the characteristics of the third zone.

The fossil ice body may be only partially involved in the main ice flow and for this reason could have a lower flow velocity. In the upper part, it was subjected to the lateral thrust of the two flow lines that caused changes in its inclination; in the lower part, the confluence of the two ice flow lines caused the total disorganization of the previous stratification and determined the compressive style of the third zone.

Finally, in Fig. 10, the isopachs of the ice cover of the central-eastern part of the glacier are mapped. The area of maximum thickness (over 80 m) corresponds to the flat zone of the bedrock. In the western part, the rough morphology of the surface did not allow the recording of data; however, these first results may be considered the beginning of a quantitative evaluation of the mass balance and glacier dynamics.

Acknowledgements. This work was carried out as part of the Programma Nazionale di Ricerche in Antartide and was financially supported by ENEA through a joint research programm on Antarctic Earth Science with the University of Siena. The authors are gratefull to G. Orombelli and C. Baroni for discussions and revision of the manuscript, and to B. Loiacono (Italian guide) for field assistance.

REFERENCES

Baroni C.; 1987: *Carta geomorfologica delle Northern Foothills nella zona della Base Italiana (Baia Terra Nova, Antartide)*. Mem. Soc. Geol. It., **33**, 195-211.

Baroni C. and Orombelli G.; 1987: *Il ghiacciaio Strandkine (Baia Terra Nova, Antartide)*. Geol. Fis. Dinam. Quart., **10**, 336-350.

Bentley C.R.; 1982: *Radar studies of Glacier Ice*. Glaciological Data, Report GD 13, 21-41.

Berry M.V.; 1975: *Theory of radio echoes from glacier beds*. Journal of Glaciology, **15**, 65-74.

Bogordosky V.V., Bentley C.R. and Gudmandsen P.E.; 1985: *Radioglaciology*. D. Reidel Publishing Company, Dordrecht, 254 pp.

Carmignani L., Ghezzo C., Gosso G., Lombardo B., Meccheri M., Montrasio A., Pertusati P.G. and Salvini F.; 1988: *Geology of the Wilson Terrane in the area between David and Mariner Glaciers, Victoria Land (Antarctica)*. Mem. Soc. Geol. It., **33**, 77-97.

Chinn T.J.H., Whitehouse I. and Hofle H.; 1989: *Report on a reconnaissence of the glaciers of Terra Nova Bay area*. Geol. Ib., **38**, 299-319.

Clough J.M.; 1977: *Radio echo sounding: reflections from internal layers in ice sheets*. Journal of Glaciology, **18**, 3-14.

Dowdeswell J.A., Drewry D.J., Lieston O. and Orheim O.; 1984: *Radio echo sounding of Spitsbergen Glaciers: problems in the interpretation of layer and bottom returns*. Journal of Glaciology, **30**, 16-21.

Harrison C.H.; 1970: *Reconstruction of subglacial relief from radio echo sounding records*. Geophysics, **35**, 1099-1115.

Harrison C.H.; 1973: *Radio echo sounding of horizontal layers in ice*. Journal of Glaciology, **12**, 383-397.

Kovacs A. and Abele G.; 1974: *Crevasse detection using an impulse radar system*. Antarctic Journal of the United States, **9**, 3-7.

Kovacs A. and Morey R.M.; 1985: *Electromagnetic measurements of multi-year sea ice using impulse radar*. In: CRREL Report 85-13, U.S. Army Corps of Eng. Hanover N.H. - U.S.A., 26 pp.

Nye J.F.; 1975: *Deducing thickness changes of an ice sheet from radio echo and other measurements*. Journal of Glaciology, **14**, 49-56.

Oswald G.K.A.; 1975: *Investigation of sub-ice bedrock characteristics by radio echo sounding*. Journal of Glaciology, **15**, 75-87.

Page D.F. and Ramseier R.O.; 1975: *Application of radar techniques to ice and snow studies*. Journal of Glaciology, **15**, 171-191.

Paren J.G. and Robin G.; 1975: *Internal reflections in polar ice sheets*. Journal of Glaciology, **14**, 251-259.

Paterson W.S.B.; 1981: *The physics of glaciers*. Pergamon Press, London, 380 pp.

Robin G.; 1975: *Radio echo sounding: glaciological interpretations and applications*. Journal of Glaciology, **15**, 49-64

Ulriksen C.P.; 1988: *Application of impulse radar to civil engineering*. Lund University of Technology, 174 pp.